

“Squaring the Circle”: Molecular Squares and Rectangles from Chelate-Induced Structural Transformations of Known Fe₁₀ and New Fe₁₂ Ferric Wheels

Theocharis C. Stamatatos,[†] Alexander G. Christou,[†] Candace M. Jones,[‡] Brian J. O’Callaghan,[‡] Khalil A. Abboud,[†] Ted A. O’Brien,[‡] and George Christou^{*,†}

Department of Chemistry, University of Florida, Gainesville, Florida 32611-7200, and Department of Chemistry and Chemical Biology, Indiana University-Purdue University Indianapolis, Indianapolis, Indiana 46202-3274

Received May 7, 2007; E-mail: christou@chem.ufl.edu

Single-strand molecular wheels¹ of paramagnetic 3d metals are of growing interest for reasons such as their high symmetry, which makes them good model systems for the study of one-dimensional magnetism,² magnetic anisotropy, and quantum effects such as coherent tunneling of the Néel vector.³ As a result, a growing number of M_x (x ≥ 8) molecular wheels are being studied. There are, however, relatively few other 3d M_x loop-like closed topologies⁴ when compared to those containing diamagnetic 4d and 5d metals such as Pd, Pt, Au, etc., or metal–metal-bonded M₂ repeating units.⁴ These span a variety of metals and ligands and have resulted in a wide range of loop and multi-loop structures, from squares, rectangles, boxes, etc., to complicated three-dimensional polyhedra.⁵ In addition to their inherent properties, such species are also potential building blocks for molecular nanodevices.⁶ Analogous access to a greater range of loop-like closed topologies for paramagnetic 3d metals would offer benefits to a variety of spectroscopic, electrochemical, magnetic, and host–guest binding studies. For this reason, we are developing the currently unexplored reactivity chemistry of 3d metal wheels, the prototype of which was the planar “ferric wheel” [Fe₁₀(OMe)₂₀(O₂CR)₁₀] (**1**).⁷ In this paper, we report a new, diolate-containing class of ferric wheel [Fe₁₂(pd)₁₂(O₂CET)₁₂] (**2**), and that N-based chelates can convert molecular wheels **1** and **2** into molecular squares and rectangles.

The reaction of [Fe₃O(O₂CET)₆(H₂O)₃]⁺ with an excess of 1,3-propanediol (pdH₂) in MeCN followed by addition of Et₂O gave yellow-green needles of [Fe₁₂(pd)₁₂(O₂CET)₁₂] (**2**) in 75% yield. Its structure⁸ (Figure 1) comprises 12 Fe^{III} atoms linked via EtCO₂[−] and pd^{2−} bridges to form a puckered wheel of crystallographic S₆ symmetry, with each η²:η²:μ₃-pd^{2−} group bridging three adjacent octahedral Fe atoms. There are two symmetry-distinct Fe···Fe pairs, with identical bridges but differing slightly in metric parameters: (A) av Fe–O = 2.001 Å, av Fe–O–Fe = 99.57°; (B) av Fe–O = 2.022 Å, av Fe–O–Fe 97.45°. Complex **2** is a member of the general [Fe_x(OR)_{2x}(O₂CR)_x] family of ferric wheels, of which **1** and [Fe₁₂(OMe)₂₄(O₂CC(OH)Ph₂)₁₂]^{9a} are the {x = 10} and {x = 12} members, respectively; complex **2** is a {x = 12, (OR)₂ = pd^{2−}} member, the first of a new class with diolate bridges. With NO₃[−] ions, it has elsewhere been shown that pd^{2−} gives [Fe₁₈(O₂CPh)₆(pd)₁₂(pdH)₁₂(NO₃)₆](NO₃)₆.^{9b}

In the absence of any significant previous reactivity studies of the ferric wheel family, other than carboxylate substitution,¹⁰ we have initiated a study of their reactions with heteroaromatic chelates such as 2,2′-bipyridine (bpy) and 2,2′:6′,2′′-terpyridine (tpy). We wondered if such relatively inflexible chelates might affect wheel curvature and/or three-dimensional shape and thus lead to new types of wheel-related products. Indeed, reaction of **2** in MeCN with 4 equiv each of tpy and NaClO₄ gave, on addition of Et₂O, yellow

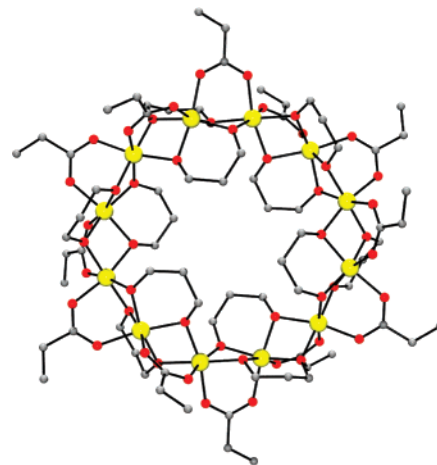


Figure 1. The structure of the Fe₁₂ ferric wheel **2**. Hydrogen atoms have been omitted for clarity. Color scheme: Fe^{III} yellow, O red, C gray.

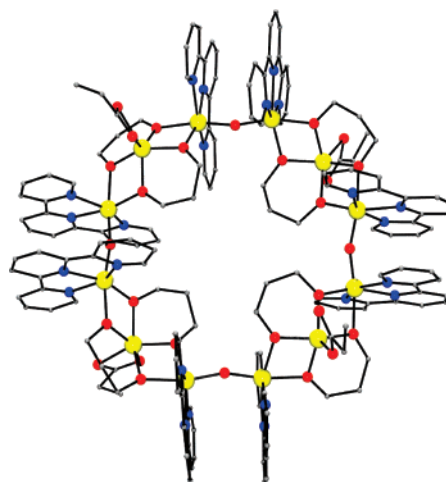


Figure 2. The structure of the [Fe₁₂]⁸⁺ cation of **3**. Hydrogen atoms have been omitted for clarity. Color scheme: Fe^{III} yellow, O red, N blue, C gray.

prisms of [Fe₁₂O₄(pd)₈(O₂CET)₄(tpy)₈](ClO₄)₈ (**3**) as **3**·10MeCN in 10% nonoptimized yield. A higher-yield procedure (~90% based on Fe) was subsequently developed from the reaction of Fe(ClO₄)₃·6H₂O with 1 equiv of tpy and a large excess of pdH₂ in MeCN. The [Fe₁₂]⁸⁺ cation⁸ of **3** (Figure 2) is a molecular square comprising alternating {Fe₂(μ-O)(tpy)₂}⁴⁺ “side” and {Fe(η²:η²:μ₃-pd)₂(η²-O₂-CET)}^{2−} “corner” subunits linked by pd^{2−} O atoms. As for **2**, the [Fe₁₂]⁸⁺ square is not planar, and the Fe–Fe distances fall into two ranges: 3.506–3.551 Å in the {Fe₂(μ-O)(tpy)₂}⁴⁺ subunits, and 3.135–3.162 Å between the latter and the {Fe(O₂CET)(pd)₂}^{2−} subunits. The Fe–O^{2−}–Fe and Fe–O(pd)–Fe ranges are 161.19–168.10 and 103.31–109.22°, respectively.

[†] University of Florida.

[‡] Indiana University-Purdue University Indianapolis.

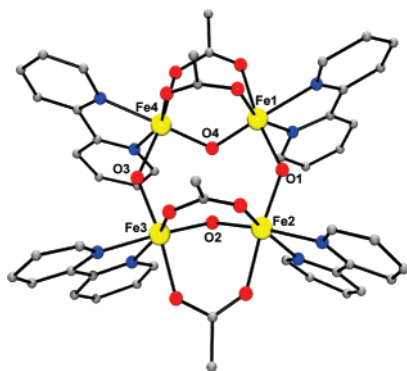


Figure 3. The structure of the cation of **4**. Hydrogen atoms are omitted for clarity. Color scheme: Fe^{III} yellow, O red, N blue, C gray.

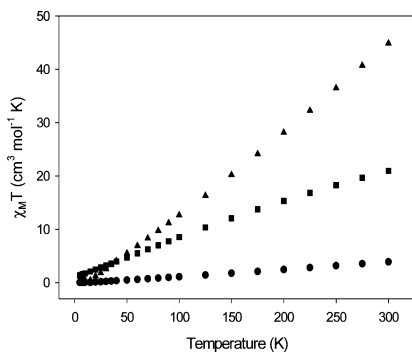


Figure 4. Plot of $\chi_M T$ versus T for complexes **1** (■), **3** (▲), and **4** (●).

Similarly, reaction of **1** ($R = \text{Me}$) in MeCN with 4 equiv each of bpy and NaClO₄ gave, on addition of Et₂O, green crystals of [Fe₄O(OH)₃(O₂CMe)₄(bpy)₄(ClO₄)₃ (**4**) in 30% yield. The structure⁸ of the cation of **4** (Figure 3) is similar to the 1,10-phenanthroline derivative¹¹ and consists of a planar Fe^{III}₄ rectangle (Fe1^{•••}Fe4 = 3.207 Å, Fe2^{•••}Fe3 3.293 Å, Fe1^{•••}Fe2 = 3.674 Å, and Fe3^{•••}Fe4 = 3.698 Å); the Fe–Fe–Fe angles are in the range of 89.30–91.08°. Three sides are bridged by OH[−] (O1, O2, O3) and one by O^{2−} (O4) ions (confirmed by bond valence sum calculations; see Supporting Information) and the short sides each also by two η¹:η¹-μ-MeCO₂[−] groups. There is an intramolecular hydrogen bond (O2^{•••}O4 = 2.523 Å) with the H atom asymmetrically located since Fe–O4 bonds (av 1.856 Å) are shorter than Fe–O2 ones (av 1.926 Å), showing that O4 retains its O^{2−} character.

Solid-state magnetic susceptibility (χ_M) data were collected on vacuum-dried, microcrystalline samples of complexes **2–4** in the 5.0–300 K range and in a 0.1 T magnetic field. In all cases, $\chi_M T$ decreases steadily with decreasing temperature from 20.96 (**2**), 44.87 (**3**), and 3.90 (**4**) cm³ mol^{−1} K at 300 K to 1.35 (**2**), 0.40 (**3**), and 0.03 (**4**) cm³ mol^{−1} K at 5.0 K (Figure 4). These indicate $S = 0$ ground states, as expected for antiferromagnetic exchange interactions between even-membered loops of Fe^{III} atoms.

Theoretical calculations were performed on **2–4** using the ZILSH method¹² to probe the strength of their exchange constants J_{ij} ($\mathcal{H} = -2J\hat{S}_i\cdot\hat{S}_j$ convention). For **2**, the two exchange constants were $J = -20.5$ cm^{−1} and $J' = -13.3$ cm^{−1} for the A and B Fe₂ pairs, respectively. For **3**, {Fe₂(μ-O)} and {Fe(μ-pd)₂} J values were in the ranges of −124.6 to −152.6 cm^{−1} and −32.1 to −49.8 cm^{−1}, respectively. For **4**, $J_{14} = -69.0$ cm^{−1}, $J_{12} = -27.0$ cm^{−1}, $J_{34} = -32.4$ cm^{−1}, and $J_{23} = -22.8$ cm^{−1} (the subscripts refer to the atom labels); these were refined by fits to the magnetic susceptibility data using a genetic algorithm method described elsewhere,¹² which gave $J_{14} = -63.3$ cm^{−1}, $J_{12} = -25.2$ cm^{−1}, $J_{34} = -26.6$ cm^{−1}, $J_{23} = -19.8$ cm^{−1}, and $g = 1.97$, with TIP fixed at 600×10^{-6} cm³

K mol^{−1}. The fit is shown in the Supporting Information. As expected, the oxide-bridged pair (Fe1^{•••}Fe4) is much more strongly antiferromagnetically coupled than the OH[−]-bridged pairs.¹³ The Fe1^{•••}Fe2 and Fe3^{•••}Fe4 couplings are similar, as expected, and J_{23} is weaker, again as expected on the basis of the smaller Fe2–O–Fe3 angle (117.5°) versus ~135° for Fe1–O–Fe2 and Fe3–O–Fe4.^{14–16} For all the compounds, the signs and relative magnitudes are consistent with established magnetostructural correlations.^{12–16}

In summary, the incorporation of inflexible bpy and tpy chelates into ferric wheel chemistry has led to products retaining a single-strand loop structure and possessing square or rectangular topologies. Of the products **3** and **4**, Fe₁₂ complex **3** more closely resembles its Fe₁₂ starting material **2**, which can be rationalized as due to the bidentate, chelating pd^{2−} being more able to resist structural disruption by the added chelate than can MeO[−] wheel **1**. In fact, **3** can be conveniently related to **2** as being the result of clipping eight tpy groups onto **2** and causing, as a consequence of the loss of the bridging carboxylate groups at these positions, formation of the near-linear Fe–O–Fe sides of a square topology. This suggests that many other interesting loop structures of various size and shape await discovery in 3d M/O chemistry by appropriate choice of the combination of bridging and chelating ligands. Further studies along these lines are in progress.

Acknowledgment. This work was supported by NSF (G.C.) and an IBM Shared University Research grant to IU (T.O'B.). C.M.J. acknowledges funding from the Undergraduate Research Opportunities Program at IUPUI.

Supporting Information Available: Crystallographic details in CIF format for **2–4**, additional structural figures, magnetic susceptibility fit for **4**, and Fe and O bond valence sums. This material is available free of charge via the Internet at <http://pubs.acs.org>.

References

- Winpenny, R. E. P. In *Comprehensive Coordination Chemistry II*; Mc Cleverty, J. A., Thomas, T. J., Eds.; Elsevier: Oxford, 2004, Vol. 7, pp 125–176 and references therein.
- Kahn, O. *Molecular Magnetism*; VCH Publishers: New York, 1993.
- Meier, F.; Loss, D. *Phys. Rev. Lett.* **2001**, *86*, 5373.
- (a) Lehn, J.-M. *Supramolecular Chemistry*; VCH Publishers: New York, 1995. (b) Fujita, M. *Chem. Soc. Rev.* **1998**, *27*, 417. (c) Leininger, S.; Olenyuk, B.; Stang, P. J. *Chem. Rev.* **2000**, *100*, 853. (d) Cotton, F. A.; Lin, C.; Murillo, C. A. *Acc. Chem. Res.* **2001**, *34*, 759.
- Yuan, Q.-H.; Wan, L.-J.; Jude, H.; Stang, P. J. *J. Am. Chem. Soc.* **2005**, *127*, 16279 and references therein.
- Stupp, S. I.; Guest Editor. Thematic Issue: Functional Nanostructures. *Chem. Rev.* **2005**, *105*, 1023.
- Taft, K. L.; Lippard, S. J. *J. Am. Chem. Soc.* **1990**, *112*, 9629.
- Crystal data for **2**: C₇₂H₁₃₂O₄₈Fe₁₂, 2436.03 g mol^{−1}, trigonal P₃¹/c, $a = 19.248(1)$ Å, $c = 17.868(19)$ Å, $\gamma = 120^\circ$, $Z = 2$, $V = 5733(7)$ Å³, $d_{\text{calc}} = 1.498$ g cm^{−3}, $T = 173(2)$ K. Final R1 = 5.19 and wR2 = 11.30%. For **3**·10MeCN: C₁₇₆H₁₈₆N₃₄O₆₀Cl₈Fe₁₂, 4691.39 g mol^{−1}, triclinic P1, $a = 19.293(7)$ Å, $b = 19.914(8)$ Å, $c = 26.176(10)$ Å, $\alpha = 85.786(9)^\circ$, $\beta = 81.646(8)^\circ$, $\gamma = 89.639(7)^\circ$, $Z = 2$, $V = 9923(6)$ Å³, $d_{\text{calc}} = 1.570$ g cm^{−3}, $T = 173(2)$ K. Final R1 = 8.67 and wR2 = 18.66%. For **4**: C₄₈H₄₇N₈O₂₄Cl₃Fe₄, 1449.71 g mol^{−1}, triclinic P1, $a = 12.696(2)$ Å, $b = 17.318(2)$ Å, $c = 18.741(3)$ Å, $\alpha = 81.343(2)^\circ$, $\beta = 77.927(2)^\circ$, $\gamma = 75.815(2)^\circ$, $Z = 14$, $V = 3885(9)$ Å³, $d_{\text{calc}} = 1.463$ g cm^{−3}, $T = 173(2)$ K. Final R1 = 7.28 and wR2 = 18.64%.
- (a) Raptopoulou, C. P.; Tangoulis, V.; Devlin, E. *Angew. Chem., Int. Ed.* **2002**, *41*, 2386. (b) King, P.; Stamatatos, T. C.; Abboud, K. A.; Christou, G. *Angew. Chem., Int. Ed.* **2006**, *45*, 7379.
- Christou, A. G.; Stamatatos, T. C.; Abboud, K. A.; O'Brien, T. A.; Christou, G. Manuscript in preparation.
- Boudalis, A. K.; Lalioti, N.; Spyroulias, G. A.; Raptopoulou, C. P.; Terzis, A.; Bousseksou, A.; Tangoulis, V.; Tchuagues, J.-P.; Perlepes, S. P. *Inorg. Chem.* **2002**, *41*, 6474.
- Cañada-Vilalta, C.; O'Brien, T. A.; Brechin, E. K.; Pink, M.; Davidson, E. R.; Christou, G. *Inorg. Chem.* **2004**, *43*, 5505.
- Gorun, S. M.; Lippard, S. J. *Inorg. Chem.* **1991**, *30*, 1625.
- Weihe, H.; Güdel, H. U. *J. Am. Chem. Soc.* **1997**, *119*, 6539.
- Werner, R.; Ostrovsky, S.; Griesar, K.; Haase, W. *Inorg. Chim. Acta* **2001**, *326*, 78.
- O'Brien, T. A.; Davidson, E. R. *Int. J. Quantum Chem.* **2003**, *92*, 294.

JA073236C